Laser **A**ssisted **RO**botic **S**urgery of the anterior **E**ye **S**egment

Project full title:	Laser Assisted Robotic Surgery of the anterior Eye Segment
Project Acronym:	LA-ROSES
Grant Agreement number:	601116
Deliverable no.:	D2.1
Title:	Surgical Method & System Architecture
Contractual Date of Delivery	31/03/2015
Actual Date of Delivery	-
Organization Short Name of Milestone Leading Partner	IFAC
Organization Short Name of Other Participants	EKY, FAST
Authors	Francesca Rossi, Bernardo Magnani, Fabio Leoni
Editors	Francesca Rossi, Bernardo Magnani, Fabio Leoni
Version	6
Tasks contributing to this deliverable	T2
Dissemination Level [1]	RE
Total number of pages (including cover page)	20

[1] Dissemination Level:
PU Public
PP Restricted to other programme participants (including the Commission Services)
RE Restricted to a group specified by the consortium (including the Commission Services)
CO Confidential, only for members of the consortium (including the Commission Services)

Version Management

Version	Date	Status	Author	Modification
1	2/02/2015	Setup	Fastenica	Creation of document
2	10/02/2015	Draft	Ekymed	Structure and initial content
3	25/02/2015	Draft	All partners	Revision/Comments
4	10/03/2015	Draft	All partners	Revision/Comments
5	20/03/2015	Draft	All partners	Revision/Comments
6	31/03/2015	Final	Ekymed	Final Revision

Table of Contents

List of acronyms

The following abbreviations are used in this report:

NIR camera: Near InfraRed camera

SWIR: Short-Wavelength InfraRed

GUI: Graphical User Interface

VS: Visual Servoing

ROS: Opensource Robotic Op-erating System

TEM*:* Transmission Electron Microscopy

Executive Summary

The present deliverable D2.1 aims to describe the LA-ROSES overall system medical, functional and technical specifications, including all the requests of the end user (surgeon). In order to extract the functional specifications and constrains of the robotic platform, the up-to-date manual laser welding procedure is first described and analyzed. These functional specifications provide designing input for the development of the LA-ROSES robotic platform capable of performing automatically, but under the supervision of the surgeon, the up-to-date manual surgery laser corneal welding process involved in keratoplasty surgical procedure. The activities here described are the result of several actions performed at the beginning of the project, starting from January 2015, and also performed during the period before the formal kick-off of the project, including the proposal preparation period.

The preliminary main activities aiming to define the technical specifications of the LA-ROSES project were:

1. an extensive literature analysis of the main publication regarding keratoplasty,
2. interviews with end-users,
3. interviews with companies in medical device ophthalmology market,
4. surgical interventions examination, both with video and in surgery rooms,
5. several consortium meetings.

1 The surgical Method

1.1 The transplant of the cornea: current techniques

The transplant of the cornea can be performed with different approaches and different surgical tools (laser assisted or manual procedure), depending on surgeon skills and patient pathology and specificity. The basic principle is to substitute the unhealthy corneal tissue (the whole cornea or a portion of it) with a donor cornea or its portion. The standard procedure is to cut the patient and donor cornea with a manual procedure, using corneal trephines, microkeratome, knives, etc. Nowadays it is also possible to perform laser assisted preparation of corneal tissue, cutting in depth different geometries and shapes, thus offering the possibility to design a "customized" surgery, tailored on patient's pathology and morphology (Yoo SH, Hurmeric V. Femtosecond laser-assisted keratoplasty. Am J Ophthalmol 2011; 151(2):189-91; Menabuoni L, Canovetti A, Rossi F, Malandrini A, Lenzetti I, Pini R. The 'anvil' profile in femtosecond laser-assisted penetrating keratoplasty. Acta Ophthalmol. 2013 Apr 26 91(6):e494-5. doi: 10.1111/aos.12144.). The prepared donor tissue is inserted in the recipient bed, substituting unhealthy tissue, and then it is typically sutured with needle and stitches in its final correct position.

Three different approaches are nowadays used in corneal transplantation: anterior lamellar keratoplasty, posterior lamellar keratoplasty (or endothelium transplant) and penetrating keratoplasty (Donald T H Tan, John K G Dart, Edward J Holland, Shigeru Kinoshita, Corneal transplantation, Lancet 2012; 379: 1749–61). Lamellar keratoplasty usually reduces the surgical and postoperative risks, resulting in better visual outcomes.

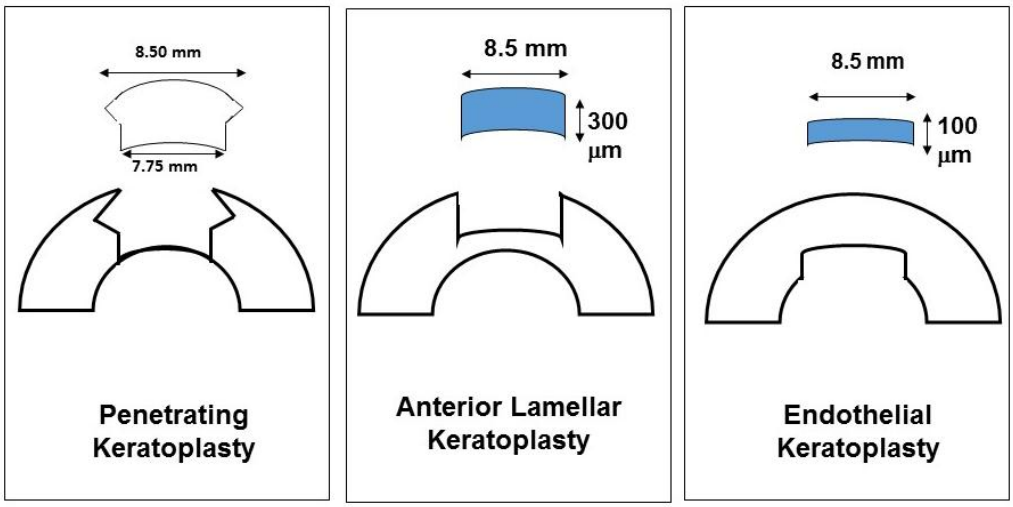

Fig. 1 - Sketches of three possible corneal transplantation geometry

In anterior lamellar keratoplasty only the external layer of the cornea is substituted. In posterior lamellar keratoplasty only the inner layers of the cornea are substituted: in this case, there is no possibility to suture the transplanted tissue, left to naturally recover; a high risk of transplanted tissue dislocation is reported in literature. Penetrating keratoplasty consists in the substitution of the whole cornea, assured in its final position with the use of suturing (needle and stitches). During the healing phase, the use of stitches can induce a deformation of the corneal curvature, due to mechanical tensions between the stitches and the healing tissue at the surgical wounds sites. This deformation results in astigmatism, so in a poor vision outcomes.

An important aspect that has to be underlined, is that corneal tissue is an avascularized tissue, so that the wound healing process is slow: transplanted tissue dislocation can be observed years after surgery (T. Nishuda, "Cornea", Chap. 1 in Cornea. Fundamentals of cornea and external disease, Vol. I, J. H. Krachmer, M. J. Mannis, E.J. Holland, Eds., pp. 3-27, Mosby, St Louis, MO (1997)).

In the last ten years laser welding of corneal tissue has been studied and proposed in order to perform laser assisted suturing of the cornea, concluding the transplant procedure. It provides an immediate closuring effect of the transplanted tissue, to stabilize the flap in its final position, avoiding mechanical tensions and deformation in the healing phase and to suture thin tissues in inaccessible sites (laser-assisted microsurgery). The proposed technique has been tested in preclinical and clinical studies (Pini R, Rossi F, Matteini P, Ratto F. Laser tissue welding in minimally invasive surgery and microsurgery. In: Pavesi L, Fauchet PM, eds. Biophotonics Series: Biological and Medical Physics, Biomedical Engineering: Springer. 2008:275-299; Rossi F, Pini R, Menabuoni L, Mencucci R, Menchini U, Ambrosini S, Vannelli G. Experimental study on the healing process following laser

welding of the cornea. J Biomed Opt 2005; 10(2):024004.; Rossi F, Pini R, Menabuoni L. Experimental and model analysis on the temperature dynamics during diode laser welding of the cornea. J Biomed Opt 2007; 12(1):014031; Luca Buzzonetti, Paolo Capozzi, Gianni Petrocelli, Paola Valente, Sergio Petroni, Luca Menabuoni, Francesca Rossi, Roberto Pini.Laser Welding in Penetrating Keratoplasty and Cataract Surgery in Pediatric Patients. Early Results. J Cataract Refract Surg 2013 Dec; 39(12):1829-34. pii: S0886-3350(13)00981-4. doi: 10.1016/j.jcrs.2013.05.046; Annalisa Canovetti, Alex Malandrini, Ivo Lenzetti, Francesca Rossi, Roberto Pini, Luca Menabuoni. Laser-assisted penetrating keratoplasty: one year's results in patients, using a laser-welded "anvil"-profiled graft. Am J Ophthalmol. 2014 Oct;158(4):664-670.e2. doi: 10.1016/j.ajo.2014.07.010).

The laser welding of corneal tissue is based on the use of a Near-Infrared (NIR) diode laser, emitting at 810 nm, and a chromophore (Indocyanine Green- ICG) that is used to stain the corneal tissue and absorb the laser light. The laser light is delivered to the target by the use of an optical fiber, manually guided by the surgeon. The critical aspects of the manual procedure are: the lack of a standard control of the light source distance from the target, resulting in different and not controlled thermal effects; the lack of a temperature control, in order to verify the efficacy and safety of the procedure; the lack of a movement control, reducing the hand tremor and monitoring the correct movement and speed of the light source. The use of a sensorized robotic interface can overcome these drawbacks related to the manual procedure.

1.2 Laser welding of biological tissues

Laser welding of biological tissues has been proposed in several surgical fields for the closure of wounds in controlled laboratory tests over the last 30 years. Joining tissues by application of laser irradiation was first reported at the end of the seventies, when a neodymium:YAG laser was used successfully to join small blood vessels (1). Since then, several experiments have been performed using a variety of lasers for sealing many tissue types, including blood vessels, nerves, skin, urethra, stomach and colon (see also previous reviews (2, 3)). Laser welding has progressively gained relevance in the clinical setting, where it now appears as a valid alternative to standard surgical techniques.

According to a general perspective, lasers hold the promise to provide instantaneous, watertight seals, which is important in many critical surgeries, as e.g. for gastrointestinal and vascular repairs, without the introduction of foreign materials, such as sutures or staples. Nowadays, due to the increasing demand for minimally invasive procedures, laser welding is emerging as the appropriate technique for applications in which suturing and stapling is particularly difficult, such as in microsurgery, laparoscopy or endoscopy, or for the treatment of extremely thin tissues. Other advantages over conventional suturing include reduced operation times, fewer skill requirements, decreased foreign-body reaction and therefore reduced inflammatory response, increased ability to induce regeneration of the original tissue architecture and an improved cosmetic appearance. The final aim of this procedure is to improve the quality of life of patients, by reduction of healing times and the risk of postoperative complications.

The laser-tissue interaction occurring during a laser-mediated welding of biological tissues is quite unanimously considered to be photothermal (2,3). This interaction is distinguished by the absorption of photons emitted by the laser source, which generates heat through a target volume. The thermal changes induced within the tissue about the lesion result, in turn, in a bond between its adjoining edges. The heat is produced through the absorption of the laser energy by endogenous or exogeneous chromophores.

In order to improve the localization of laser light absorption, the application of photo-enhancing dyes to the tissue has been proposed. These exogenous optical chromophores have enabled the fusion of wounds selectively and at low irradiation fluences, thus reducing the risk of excessive thermal damage to surrounding tissues. In fact, acting as wavelength-specific absorbers, they make it possible to achieve differential absorption of the laser light between the stained region and the surroundings. In practice, while the usage of a wavelength strongly absorbed by the endogenous chromophores induces very high temperature values in the area under direct irradiation, the combination of a proper exogenous chromophore and a laser wavelength at which the tissue is almost transparent allows for a confined and homogenous temperature enhancement deep in the stained tissue. The resulting welding effect may be modulated in the depth of the tissue, thus resulting in a more effective closure of the wound. Various chromophores have been employed as photo-enhancing dyes, including indocyanine green (ICG), fluorescein, basic fuchsin, and India ink (4,5). A very popular setting of tissue laser welding includes the use of a near-infrared laser, which is poorly absorbed by the biological tissue, in conjunction with the topical application of a chromophore absorbing in the same spectral region. Current examples of this modality are in the transplant of the cornea, in cataract surgery, in vascular tissue welding, in skin welding and in laryngotracheal mucosa transplant (4,6,7). In all these cases diode lasers emitting around 800 nm and the topical application of ICG have been used.

1.3 Mechanism of thermal laser welding

Understanding the mechanism responsible for the sealing process mediated by laser light is important for the appropriate selection of laser parameters (power density, pulse duration and spot size) for the tissue to be welded. In this way, a combination of maximal bonding strength and minimal thermal damage can be achieved. According to the current understanding and interpretation, laser welding is a soft thermal treatment of wound edges in which laser radiation is absorbed by the tissue, either directly from its principal absorbers such as water, or from exogenous chromophores applied topically to the wound area. In the heated tissue the main components undergo thermal modifications, resulting into the fusion of the apposed flaps.

1.3.1 Composition of the extracellular matrix

The main components of the extracellular matrix of biological tissues include proteins, mainly collagen, and nonproteic material, which is principally constituted of proteoglycans and glycosaminoglycans.

Collagen is the most abundant protein in the body and the main component of connective tissues. This protein has a triple helix composed of polypeptide chains highly stabilized by interconnecting hydrogen bonds. Within the collagen family, the main component of fibril-forming collagens is type I collagen, which provides the structural and organizational framework for the cornea and other tissues. In this type of collagens, molecules are packed in a quarter-staggered manner and connected by covalent bonds to form microfibrils a few nanometers in diameter, which then combine to form collagen fibrils of about 30 nanometers in size. The regular arrangement of the collagen molecules gives rise to a structural periodicity along the microfibrils and fibrils with a repeated distance of 65-67 nm. This periodicity results in a cross striations pattern that is apparent under electron microscopy. The absence of this pattern indicates a loss in the spatial organization within the collagen fibrils and is often used as a marker for the onset of thermal denaturation.

In connective tissues, collagen fibrils and interfibrillar proteoglycans (PGs) form a dense and well-organized mutually interconnecting network. The interfibrillar PGs usually display a globular protein part (head) to which one glycosaminoglycan (GAG) is attached (tail). The interfibrillar PGs constitute a well-defined, complex molecular chain system providing rigid bridges between the fibrils and thereby being responsible for the maintenance of the regular array of collagen fibrils. PGs are equidistant and orthogonally attached at specific sites of the collagen fibrils by their protein cores. The interaction of the PGs with the collagen fibrils is thought to be noncovalent and is characterized by a high affinity constant. By using a specific proteoglycan staining for electron microscopy, GAGs have been shown to form antiparallel doublets (dimers) which make it possible to maintain the relative positions among the adjacent collagen fibrils (8). According to Scott's hypothesis, two GAG chains, one from each PG, form duplexes, covering the space between fibrils, anchored by protein cores attached to each fibril (8,9). In a recent paper a multifaceted analysis has brought to light that the model GAG, hyaluronan, can generate stable aggregates (polymer networks) in physiological solution (10). These structures can be dissolved reversibly upon heating at temperatures exceeding 40°C. This led to hypothesize the formation of junction zones mediated by weak heat-labile interactions, partly confirming Scott's hypothesis.

1.3.2 Thermal modifications of connective tissues and mechanism of welding

When a connective tissue is subject to a temperature rise, several morphological changes occur to its extracellular components. The first step is governed by the thermal denaturation of PGs mainly occurring before the onset of fibrillar collagen denaturation, i.e. from ~45 to ~60°C. In this range one or two subsequent phase transitions are observed which are correlated to a local disorder of the regular fibrillar collagen arrangement. Likely this is ascribed to the breaking of interfibrillar PGs bridges, which leads to a drastic change of the interfibrillar distances (10,11). The next stage consists in the helix-to-coil transition of collagen molecules which proceeds in two following steps. At first, unwinding of the triple helices occurs due to the hydrolysis of the intramolecular hydrogen bonds. This leads to tissue shortening and to a loss of periodicity due to a shrinkage effect parallel to the axis of the fibrils (12). As a consequence, fibrillar edges appear frayed and the average fibrillar diameter increases. At higher temperatures covalent cross-links connecting collagen strands break, resulting in a complete destruction of the fibrillar structure and causing full denaturation of collagen and relaxation of the tissue (13). The onset of collagen shrinkage often quoted in the clinical literature is around 60°C, while relaxation is reported to occur beyond 75°C (14). However, it is worth noting that collagen denaturation is a rate process governed by the local temperature/time response: thus the time/temperature profile influences the shrinkage threshold of collagen, as well as the relaxation phase (15). Moreover, both the temperature for maximum shrinkage and the relaxation temperature depend on the cross-links density which rises on tissue ageing as well as on hydroxyproline (one of the main amino acids constituting the collagen backbone) content which varies among species and tissues.

The modifications occurring to collagen and proteoglycans upon photothermal laser treatment have been mainly monitored by means of different microscopy techniques. These include traditional methods as optical and fluorescence microscopy which allow for an investigation at the micron scale (16) and transmission and scanning electron microscopy (TEM and SEM, respectively) which are useful when studying nanometric structures (11, 17, 18). Other techniques recently applied for the analysis of biological material have also been tested, such as atomic force microscopy (AFM) and second-harmonic generation (SHG) microscopy which provide complementary information (19-21). These studies have been helpful (although not exhaustive) in elucidating the different dynamics behind the sealing process.

According to the scientific literature, different schemes can be invoked for the laser welding of biological tissue. At first, by considering the effects induced by the photothermal treatment, we can distinguish a "hard", a "moderate" or a "soft" laser tissue welding. In other words, on the basis of the dosimetry of the laser irradiation, the choice of the laser and the parameters setting, the tissue type and the nature of the absorber (endogenous or exogenous), different dynamics of the extracellular matrix develop at the weld site. These can be typically distinguished in: 1) the photocoagulation of the collagen, 2) the "interdigitation" of collagen fibrils and 3) the reorganization of the nonfibrillar components, which are associated with the "hard", the "moderate" and the "soft" laser welding, respectively.

The soft laser welding is the effect that is used to support suturing in penetrating keratoplasty.

1.3.3 Soft laser welding

A secondary role of fibrillar type I collagen in the laser welding mechanism has been pointed out in some recent studies, suggesting the involvement of some other extracellular matrix components. In these studies a combination of a low power NIR laser operated in CW mode and the topical application of NIR-absorbing dyes has been proposed for the welding of corneal tissue (6, 11, 21). Microscopy data revealed groups of interwoven fibrils joining the sides of the cut at the weld site. In particular, transmission electron microscopy and atomic force microscopy analyses clearly indicated that type I collagen was not denatured at the operative laser energy densities employed (21). The preservation of substantially intact, undenatured collagen fibrils in laser-welded corneal wounds finds consistency with previous thermodynamic studies, which revealed temperatures below the denaturation threshold of fibrous collagen under laser irradiation.

Most likely the use of a chromophore was responsible for a controllable temperature rise confined to the area where it had been previously applied, in turn resulting in a "soft" thermal effect. In the case of low-temperature laser welding, a different model of the sealing process must be invoked. The GAGs bridges connecting collagen fibrils in the native tissue are probably broken at the characteristic temperatures of diode laser welding (in the 50-65°C range). The individual GAG strands, freed upon heating, subsequently create new bonds with other free strands during the cooling phase. In practice, the interwoven fibrils observed at the weld site are supposed to be connected by several newly-formed GAG bridges. The possibility of a "soft" laser welding mechanism not involving the fibrillar collagen finds also agreement with earlier studies on welded tissue extracts analyzed by gel electrophoresis (22-25).

1.4 Surgical applications of thermal laser welding

To the best of our knowledge, the technique proposed in LA-ROSES experiment is the only one laser welding application which have reached the preclinical and clinical phases. It is based on the use of a near infrared diode laser emitting at 810 nm and the topical application of the chromophore ICG, which shows high optical absorption at the laser wavelength emission (26-29). The procedure consists in a preliminary staining phase with the chromophore, followed by an irradiation phase. ICG has been chosen because of its biocompatibility which has already favored its exploitation in several biomedical applications. In practice, the chromophore is prepared in the form of an aqueous saturated solution of commercially available Indocyanine Green for biomedical applications (e.g. IC-GREEN Akorn, Buffalo Grove, IL or ICG-Pulsion Medical Systems AG, Germany). This solution is accurately positioned in the tissue area to be welded, using particular care to avoid the staining of surrounding tissues, and thus their accidental absorption of laser light. Then the wound edges are approximated and laser welding is performed under a surgical microscope.

The laser used in preclinical tests and in the clinical applications is typically an AlGaAs diode laser (e.g Mod. WELD 800 by El.En. SpA, Italy) emitting at 810 nm and equipped with a fiberoptic delivery system.

In penetrating keratoplasty, the optimized technique has been named the continuous wave laser welding (CWLW). Non-contact, CW diode laser irradiation is used for the welding of corneal wounds, in substitution or in conjunction with traditional suturing procedures. Surgical procedures, thermal modeling, as well as microscopic

analyses in the case of CW diode laser welding have been widely reported (6,11,26-29) . The CWLW is based on the “soft” laser welding effect, as described in the former paragraphs.

1.4.1 Laser welding in Ophthalmology

The first clinical application of laser closure of ocular tissues was in the treatment of corneal surgical wounds, in which the requirement of an immediate, watertight seal appears very useful in performing advanced ophthalmic surgeries, as well as in the treatment of accidental traumas and perforations. The development of a minimally invasive laser welding technique of transparent ocular tissues may potentially allow for the recovery of a good vision in a short post-operative time, by providing better stability of laser-welded wounds, with minimal inflammation and greater protection from infections. This could ultimately result in a better quality of life of patients and reduce hospitalization costs.

Clinical activity on the use of CWLW were carried out by Menabuoni and co-workers at the Ophthalmic Department of the public hospital of Prato, Italy (upon approval of the Ethical Committees of the Local Health Board). The main clinical applications of CWLW are in cataract surgery, in penetrating keratoplasty (i.e. full thickness transplant of the cornea) and in lamellar keratoplasty (partial thickness transplant of the cornea). An improvement in lamellar and penetrating keratoplasty was performed by integration of the diode laser welding procedure in combination with the femtosecond laser sculpturing of corneal flaps, thus effectively optimizing the process for a precise and minimally invasive surgical transplant.

The CWLW procedure developed to weld human corneal tissues in penetrating keratoplasty is as follows. The donor and recipient cornea are trephined either mechanically or by use of a femtosecond laser, as suggested by the surgeon experience and the patient needs. The donor cornea is then applied onto the recipient eye and secured by 8-16 interrupted stitches or contininuos suturing. Then laser welding is performed all around the perimeter of the corneal. To this aim, the chromophore solution (ICG in sterile water, 10% w/w) is placed inside the corneal cut, using an anterior chamber cannula, in an attempt to stain the walls of the cut in depth. A bubble of air is injected into the anterior chamber prior to the application of the staining solution, so as to avoid perfusion of the dye. A few minutes after the application, the solution is washed out with abundant water. The stained walls of the cut appear greenish, indicating that ICG has been absorbed by the stromal matrix. Lastly, the whole length of the cut is subjected to laser treatment. Laser energy is transferred to the tissue in a non-contact configuration, through a 300-μm core diameter fiber. A typical value of the laser power density used clinically is around 10 W/cm^2, which results in a good welding effect. During irradiation, the fiber tip is kept at a working distance of about 1 mm, and at an angle of 20° - 30° with respect to the corneal surface (side irradiation technique). This particular fiber position provides in-depth homogenous irradiation of the wound and prevents accidental irradiation of deeper ocular structures. The fiber tip is continuously moved over the tissue to be welded, with an overall laser irradiation time of about 120 s for a 25-mm cut length (the typical perimeter of a transplanted corneal button). This procedure has been performed up to now on 300 patients with very satisfactory results (29, 30). The position of the apposed margins has been found to be stable over time, thus assuring optimal results in terms of postoperatively induced astigmatism after cataract and keratoplasty surgery. The lower number of stitches reduces the incidence of foreign body reactions, thus improving the healing process. Objective observations on treated patients have proved that the laser-welded tissues regain a good morphology (without scar formation) and pristine functionality (clarity and good mechanical load resistance).

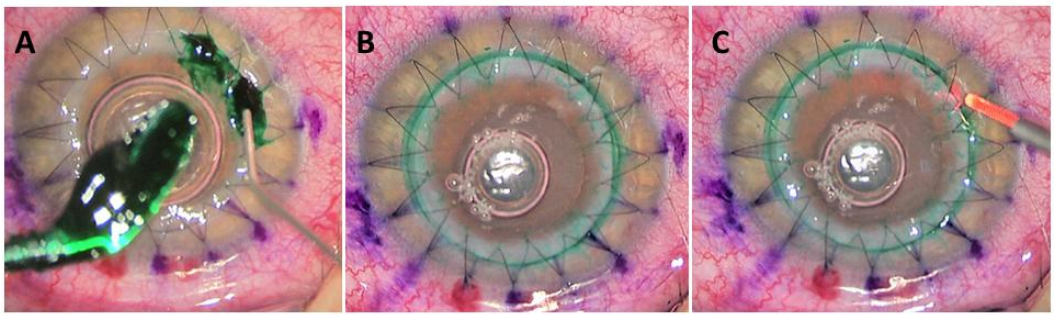

Fig. 2 - Laser assisted procedure in penetrating keratoplasty (see ref 30)

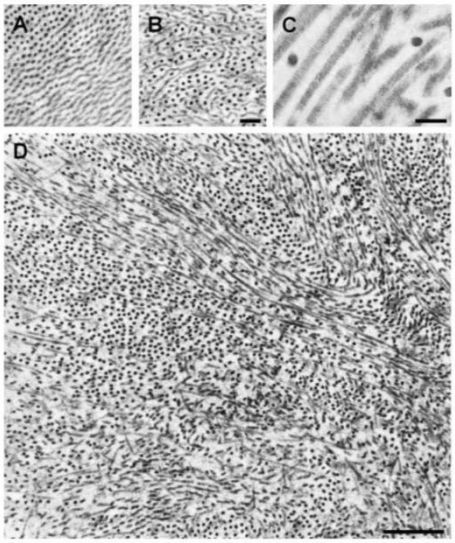

Fig. 3. TEM micrographs showing the fibrillar arrangement observed (A) in a control corneal stroma, (B) in the periphery of the cut of a welded cornea, and (C,D) at the weld site. Cross striation of fibrils is still observable after the laser treatment (C). (A,B: bar 200 nm, C: bar 100 nm, D: bar 500 nm).

Fig. 3 - TEM analysis on a laser welded cornea from ref. 11. The study was performed ex vivo on porcine corneas.

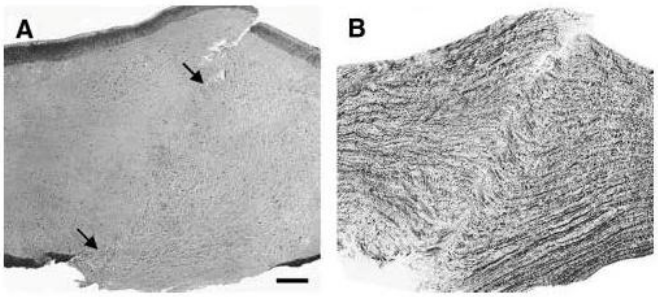

Fig. 1. Microscopic examination of diode laser-welded corneal stroma (bar 100 μm). A: Hematoxylin-eosin stain revealed absence of tissue coagulation or charring at the welded site (between the arrows). B: Negative image of the same sample stained with picrosirius red dye shows bridging structures across the wound. The birefringence signal appears more diffused at the weld site but with an intensity comparable to the one of laser-untreated regions.

Fig. 4 - Microscopy on a laser welded cornea from ref. 11. The study was performed ex vivo on porcine corneas.

2 System Architecture

Taking into account the description of the manual laser welding procedure given in the previous section, we are able to provide a list of the functional requirements we are going to implement:

- enabling circular movement of a laser probe allowing a tracking of the circular path marked by the indocyanine solution
- enabling detection of the corneal tissue at the level of the wound caused by the laser spot in order to assure a perfect tissue welding result induced by the photothermal effect
- enabling detection of the wound boundary with automatic tracking movement of the laser spot
- enabling changing laser orientation, altitude from the corneal wound and tracking velocity during the welding procedure
- enabling initial gross and accurate positioning of the laser probe above the patient's eye
- accurate laser probe positioning above the patient's eye

All above functional requirements represented designing input for the identification of a set of sub-systems able to implement some of these functionalities:

- the Eye hand-piece sub-system, comprising:
  - the laser probe
  - an infrared circular illumination system to be positioned above the patient's eye in order to enhance a visual contrast between the cornea circular wound and the iris
  - a vision sub-system comprising:
    - a NIR/SWIR camera enabling the detection of the cornea circular wound, the detection of the laser beam profile and the laser spot
    - a thermal camera for monitoring the tissue heating process induced by the photothermal effect caused by the persistence of the laser spot
  - a mechatronic system composed of an annular guide enabling radial and circular movements of the laser source. The laser beam should be free to change its orientation in order to set the best orientation according to the type of corneal cut shapes.
- a robotic arm for gross and accurate positioning above the patient's eye of an end-effector carrying all above instrumentation

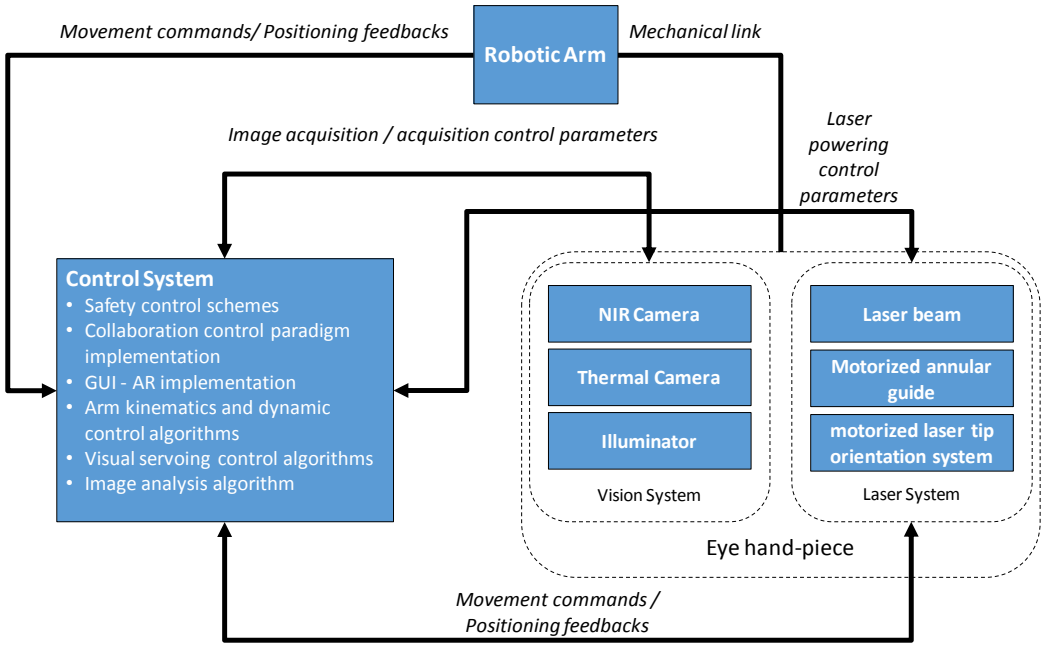

Fig. 5 - Overall system diagram

2.1 System at a glance

The LA-ROSES System consists of three main systems and other sub-systems, as follows:

- the 7 DOF robotics arm
- the Eye hand-piece system, comprising:
    - the vision system
    - the laser probe
    - the orienting mechanisms
    - the visual interface and the control system.

A preliminary sketch of the overall system is shown in the following picture

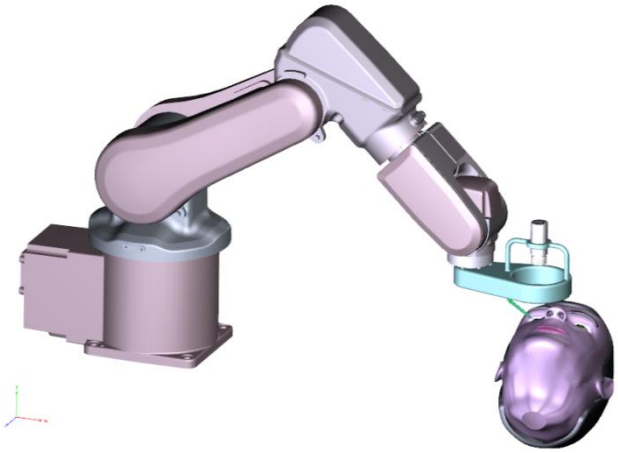

Fig. 6 - A first representation of the LA-ROSES system. The robotic arm here depicted provides a concept skeletonization only. The real arm used for the project implementation is the SCHUNK LWA 3 arm described elsewhere in this document.

The following picture represents the preliminary sketch of the Eye hand-piece sub-system.

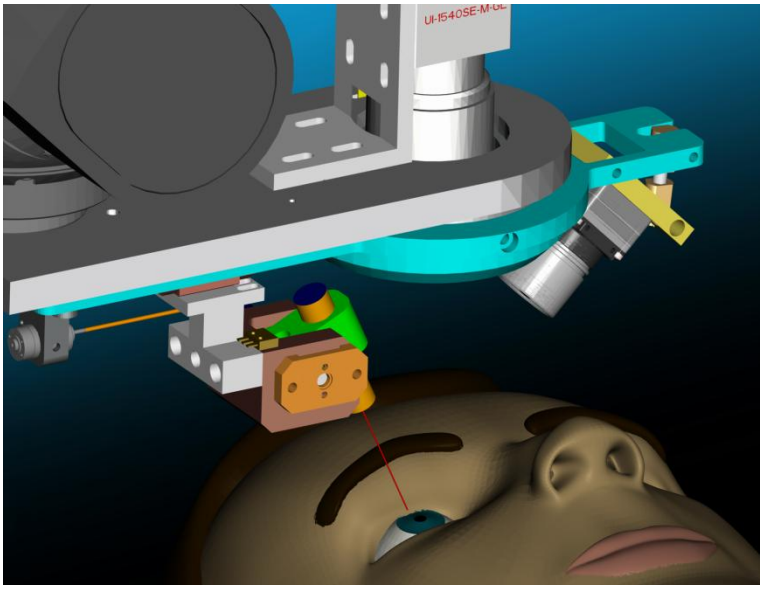

Fig. 7 - Eye hand-piece sub-system

2.2 The robotic arm

A robotic arm will be used to move the eye hand-piece system carrying cameras, lasers and the laser handling system. The selected arm is the SCHUNK Light Weight Arm (LWA3) providing 6 Degree Of Freedom (DOF) having 6 rotational joints as shown in fig. Fig. 7. The arm is controlled via a computer with a CAN bus interface operating at 500kbits/s. Both the logic unit and the actuators of the arm are powered using 24VDC. The communication protocol of the arm provides a large number of commands for configuration and motion of the arm. Two of the most relevant commands for visual servoing purposes are the position retrieval command and the velocity motion command. The first returns the angle value of a particular joint with floating point precision, which is required for calculation of the jacobian matrix and the forward kinematics of the robot, while the latter sends a signal to the low level actuator controllers to move the joint at a constant velocity specified by the command. We

choose this type of robotic arm due to its lightweight, compactness and multipurpose application possibilities covering various areas in robotics: inspection systems, service robotics, human-machine-interaction and its utilization on mobile platforms are just some examples. The joints are swivel units PRL of the PowerCube series with integrated motor-controller unit and continuous center bore for the cable feed-through form its base. The eye hand-piece will be the “end-effector” of this robotic arm and will be attached to the last joint as to be the wrist.

The robot control system will consists in the extension of the Opensource Robotic Op-erating System (ROS). ROS provides software for communicating with the SCHUNK LWA modules, but it was lacking the necessary capabilities for robot control. Then, we decided to follow ROS paradigm and contribute with new code by creating a stack to realize direct and inverse kinematic control for the gross and fine positioning of the eye hand-piece above the patient’s eye.

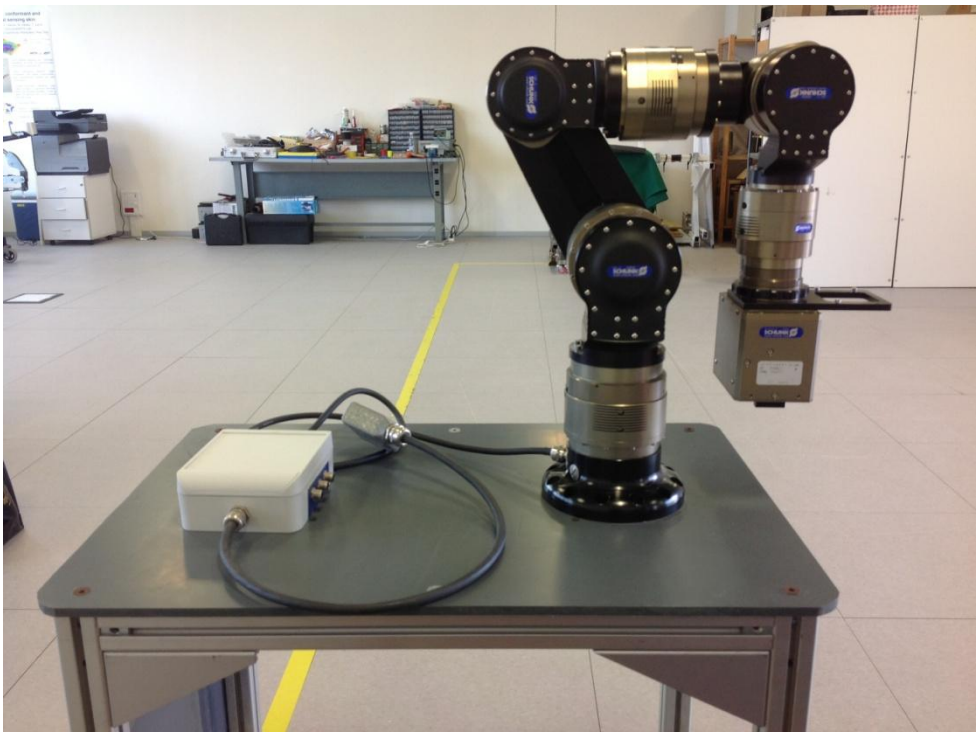

Fig. 8 - SCHUNK LWA robotic arm consisting of 6 DOF

2.3 The Eye hand-piece system

The Eye hand-piece system is the core of the LA-Roses System, it is responsible for the orientation and rotation of the laser system along the trajectory represented by the ICG chromophore, according to the cut shape chosen by the surgeons and controlled by the information of the Vision system.

It has several functions:

1. to adjust angle and distance from the laser source to the cornea
2. to rotate the laser around the corneas to be welded
3. to carry on board the vision system.

The Eye hand-piece system scheme is represented in the following picture.

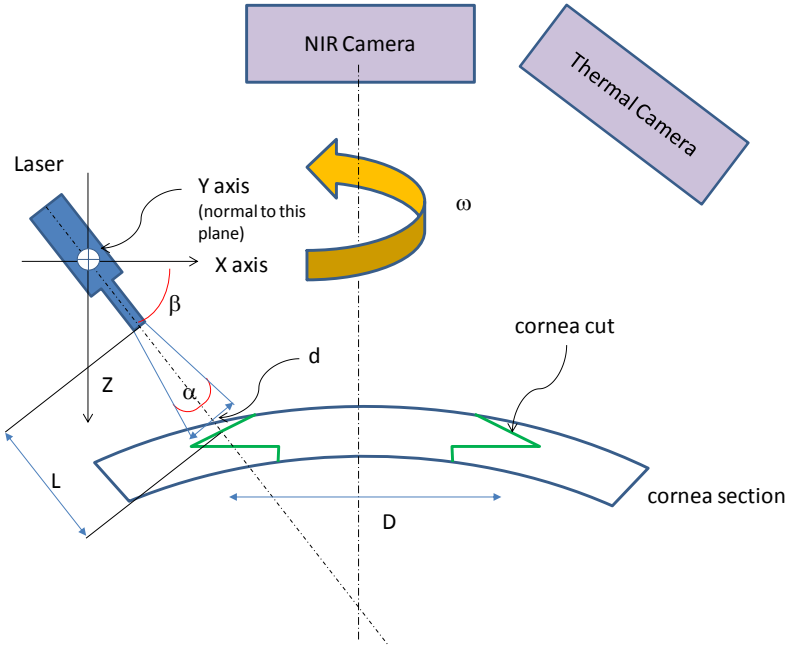

Fig. 9 - Eye hand-piece system geometrical scheme.

Where:

Z = vertical axis. Simple geometrical relations link the "z" position with X and α.

X = horizontal axis. The movement along this axis is assured by a step motor and a linear slider, with a resolution of at least 0,01 mm.

α = laser beam aperture angle

β = tilt laser beam angle

ω = axial rotation

D = average diameter of the transplanted tissue (min: 7 mm, max: 9 mm)

d = laser beam diameter.

L = laser source working distance. The nominal value is 2 mm, but the distance can be in the range 1÷3 mm. The laser spot diameter at the target depends on the working distance and the numerical aperture of the optical fibre according to this relation: $d/L = tg\ \alpha/2$.

The movements of the Eye hand-piece system are listed in the following Tab. 1.

N.	Type of movement	Ref Axis	Tasks to be accomplished	Min- Max value
1	Translation	X	• to adjust the "D" diameter of the cornea also during the rotation of Z1 axis	0 - 26 mm
2	Rotation	Y (α angle)	• to adjust the angle of incidence of the laser beam, according to the cut shape of the cornea • to maintain the laser working distance of 50 mm	25° - 65°
3	Rotation	Z_1 (ω angle)	• to assure the welding of the entire circumference of the cornea	0° - 360°
4	Translation	Z	• to maintain the laser working distance of 50 mm • to maintain the laser working distance of 50 mm	0 - 26 mm

Tab. 1 - list of movements

The following table shows the main critical components of the Eye hand-piece excluding the two vision system, described in the paragraph 2.4 and the Laser system described in the paragraph 2.5.

N.	Name	Type of actuator/model	Mechanical max resolution	With dedicated control board max resolution
1	motor 1	Step motor model Fahulhaber AM1020 V-6-65	0,11	0,0004 mm
2	motor 2	Step motor model Fahulhaber AM1020 -6-65 and Gear box ratio 1/4096	0,004°	0,000015 °
3	motor 3	Step motor model RDM66200	1,8°	0,007 °
4	motor 4	Assured by robot	0,01 mm	-

Tab. 2 - List of main components & resolutions

The positioning of the Eye hand-piece system is mainly dependent by the cornea cut shape (see for details paragraph 1). The surgeon, according to the patient pathology, decides a suitable cutting shape and the laser beam inclination (angle α), taking also into account the shape and dimension of the nose: depending on the anatomy of the patient face, not all α angle are possible, as depicted in the next picture. This problem is not strictly dependant by the LA-ROSES System: also in traditional interventions, patients with "big noses" always represent a problem for the surgeon.

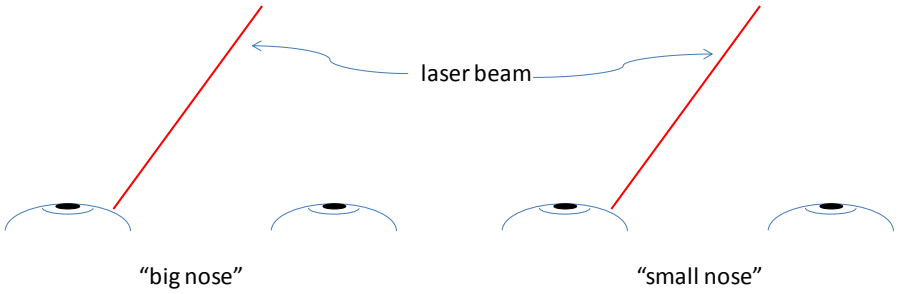

Fig. 10 - "big" and "small" patient nose.

The laser beam has also a pointer that can be used for a simulation of its trajectory before starting the surgical procedure: this is not related on possible damage on the patients skin (power Laser output is safe for the patient skin), but to avoid the possibility to not weld the entire circumference of the two tissues (donor and patient), in case the laser is "obscured" by the nose.

At present, the chosen components can assure a theoretical mechanical resolution of ± 0,001 mm.

2.4 The vision system

Generally speaking, a "vision system" comprises a set of HW devices and SW algorithms enabling images acquisition and processing in order to extract useful data from the images which are further used by another (other) system(s) to accomplish the required task(s). The LA-ROSES vision system HW devices consist of:

- Illumination system. The illumination system has to properly illuminate the patient's eye in order to enable the detection of the pupil region and enhance the recognition of the corneal wound edges. A low-power IR illumination system will be used.
- NIR Camera including lenses and optic filters
- Thermal camera including lenses and optic filters

All these devices have to be mounted onto the eye hand-piece under designing as described in Task 3. Careful selection of the illumination system has to be provided, in order to select the best method to help the development of eye tracking, by using images gathered from the NIR camera, both during the initial set-up phase and during the suturing procedure for monitoring and eventually adjust the laser beam movements according to the recorded eye movements. In general, there are two types of eye tracking techniques: bright-pupil and dark-pupil. The difference between this two is based on the location of the illumination source with respect to the optics. If the illumination is coaxial with the optical path, then the eye acts as a retroreflector as the light reflects off the retina creating a bright pupil effect similar to red eye. If the illumination source is offset from the optical path, then the pupil appears dark because the retroreflection from the retina is directed away from the camera.

Further investigations have to be done in order to select the best method suitable to be adopted in the LA-ROSES context; a complete analysis and description will be given.

The images acquired by the NIR camera are also processed in order to extract the laser beam profile (pointing direction) and the location of the laser spot projected onto the patient's eye anterior external surface. At the beginning of the suturing procedure the eye hand-piece has to be accurately positioned by using the robotic arm above the patient's eye. In order to accomplish this task the development of autonomously algorithms to perform robotic arm movements using a vision guided robotics approach is required. Using visual feedback to control a robot is commonly termed Visual Servoing (VS). Thus, machine vision or image processing are part of the vision system. Image processing techniques are required to acquire, filtrate and detect the target position inside images acquired by the NIR camera. This sequence is repeated over the time, enabling a tracking and control closed-loop scheme. Based on this sensory input, a control sequence is generated. In addition, the system may also require an automatic initialization which commonly includes figure–ground segmentation and object recognition. A typical VS task uses image information to measure the error between the current location of the robot and its reference or desired location. Images acquired from the thermal camera will be used to detect the local corneal tissue temperature in correspondence of the laser spot, so that the laser beam is moved along the welding trajectory as the desired correct temperature is reached.

2.5 The laser system

The laser used in the preclinical and clinical test is an AlGaAs diode laser (produced by EL.EN. spa, Calenzano, Italy), emitting at 810 nm, with a maximum power output of 10 W. The device was enclosed in a compact cabinet, 24x18x36 cm (see Fig. Fig. 11) and equipped with a fiber optic delivery system employing fibers with 300-µm-core diameters. Each fiber terminated in a hand piece, which enabled easy handling under surgical microscope.

Emission wavelength	810 ±10 nm
Output power	0.5-10 W *
Type of emission	CW and pulsed
Repetition rate (pulsed)	0.5-500 Hz
Power emission stability	±20 %
Aiming beam	635 nm, 1 mW
User interface	Touch screen LCD
Size	24x18x36 cm

* 50-1000 mW with the 1/10 optical attenuator accessory

Fig. 11 - The diode laser currently in use for laser welding of the cornea (left), the fiber tip mounted in a handpiece (right).

The laser has a user interface: it is possible to set different treatment duration and power.

In a preliminary configuration, the optical fiber will be mounted in the eye hand piece. Another possible configuration is currentlu under study, using a laser directly mounted in the eye hand-piece (see fig.5). It seems that the miniaturization of such a diode laser with this requirement of power and target dimension is a technological challenge, that we have to face in the framework of this project.

2.6 The control system

The robotic platform will provide a graphical user interface (GUI) allowing the surgeon to operate from a remote console. The surgery procedure will start enabling the control system of the robotic arm to adjust the position and the orientation of the suturing end-effector just above the patient's eye. The suturing end-effector consists of a diode laser source emitting a coherent light at 810nm mounted on a mechatronic device allowing the laser beam free to move following the welding trajectory. The suturing end-effector will be autonomously positioned by the robotic arm by using a Visual Servoing (VS) control scheme. The VS consists of a set of image processing algorithms able to extract useful information from images acquired by the on-board cameras (hyperspectral and thermal) in order to control the robot movements allowing a fine positioning of the suturing end-effector. Soon after the positioning procedure conclusion, the control system will detect and calculate the

welding (or suturing) trajectory; then all the system parameters related to the welding process will be proposed to the surgeon check, before enabling the start command.

However, the corneal welding task will not be fully autonomously executed by the robotic platform control system: the surgeon will have a direct control of the surgical procedure. To realize this, we chose a collaborative robot control paradigm, consisting of providing continuously information about current measurement data to the operator whilst the system performs the current task. This is what is common called an augmented reality typical scenario: the operator (surgeon) can check and supervise the running task in order to modify or adjust the robot movements if needed. In fact, a human expert like a surgeon is, is more capable to handle unexpected scenarios, as opposed to an autonomous robot; at the same time, the robot control system could autonomously decide to stop the task in case of coming out about dangerous situations to preserve patients' health.

A possible first mockup of the LA-ROSES GUI is shown in Fig. 12.

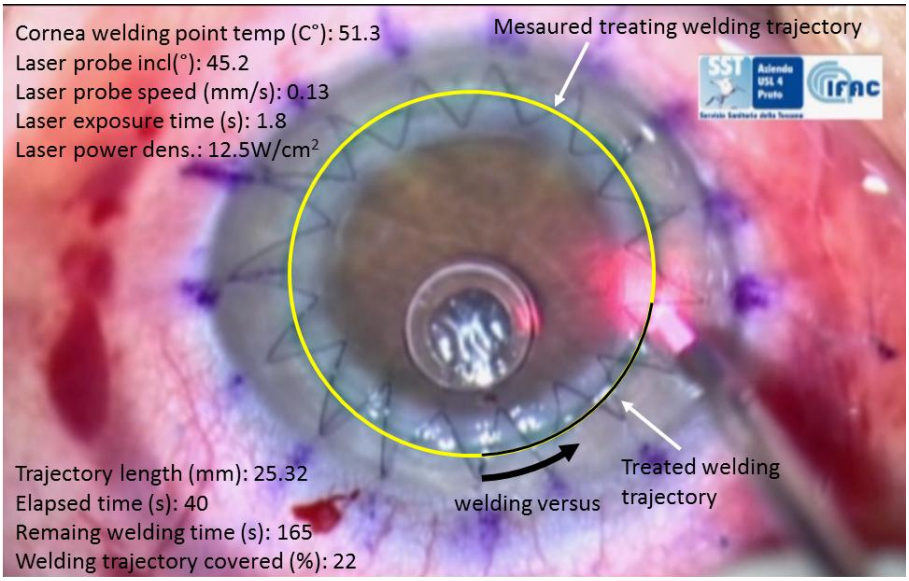

Fig. 12 - LA-ROSES GUI prototype

3 References

3.1 References of paragraphs 1.2, 1.3, 1.4

1. Jain KK, Gorisch W. Repair of small blood vessels with the neodymium-YAG laser: a preliminary report. Surgery 1979; 85(6):684-688.
2. McNally KM. "Laser tissue welding" Chap. 39. In: Vo-Dihn T, ed. Biomedical Photonics Handbook: CRC Press, Boca Raton. 2003:1-45.
3. Pini R, Rossi F, Matteini P, Ratto F. Laser tissue welding in minimally invasive surgery and microsurgery. In: Pavesi L, Fauchet PM, eds. Biophotonics Series: Biological and Medical Physics, Biomedical Engineering: Springer. 2008:275-299.
4. DeCoste SD, Farinelli W, Flotte T, Anderson RR. Dye-enhanced laser welding for skin closure. Lasers Surg Med 1992; 12(1):25-32.
5. Poppas DP, Scherr DS. Laser tissue welding: a urological surgeon's perspective. Haemophilia 1998; 4(4):456-462.
6. Rossi F, Pini R, Menabuoni L, Mencucci R, Menchini U, Ambrosini S, Vannelli G. Experimental study on the healing process following laser welding of the cornea. J Biomed Opt 2005; 10(2):024004.
7. Ott B, Zuger BJ, Erni D, Banic A, Schaffner T, Weber HP, Frenz M. Comparative in vitro study of tissue welding using a 808 nm diode laser and a Ho:YAG laser. Lasers Med Sci 2001; 16(4):260-266.
8. Scott JE, Haigh M. Identification of specific binding sites for keratan sulphate proteoglycans and chondroitin-dermatan sulphate proteoglycans on collagen fibrils in cornea by the use of cupromeronic blue in 'critical-electrolyte-concentration' techniques. Biochem J 1988; 253:607-610.
9. Scott JE. Morphometry of Cupromeronic blue-stained proteoglycan molecules in animal corneas, versus that of purified proteoglycans stained in vitro, implies that tertiary structures contribute to corneal ultrastructure. J Anat 1992; 180:155-164.
10. Matteini P, Dei L, Carretti E, Volpi N, Goti A, Pini R. Structural behavior of hyaluronan under high concentration conditions. Biomacromolecules 2009; 10:1516-1522.
11. Matteini P, Rossi F, Menabuoni L, Pini R. Microscopic characterization of collagen modifications induced by low-temperature diode-laser welding of corneal tissue. Lasers Surg Med 2007; 39:597-604.
12. Allain JC, Le Lous M, Cohen-Solal L, Bazin S, Maroteaux P. Isometric tensions developed during the hydrothermal swelling of rat skin. Conn Tissue Res 1980; 7:127-133.
13. Le Lous M, Flandin F, Herbage D, Allain JC. Influence of collagen denaturation on the chemorheological properties of skin, assessed by differential scanning calorimetry and hydrothermal isometric tension measurement. Biochim Biophys Acta 1982; 717:295-300.
14. Kampmeier J, Radt B, Birngruber R, Brinkmann R. Thermal and biomechanical parameters of porcine cornea. Cornea 2000; 19(3):355-363.
15. Brinkmann R, Radt B, Flamm C, Kampmeier J, Koop N, Birngruber R. Influence of temperature and time on thermally induced forces in corneal collagen and the effect on laser thermokeratoplasty. J Cataract Refract Surg 2000; 26:744-754.
16. Savage HE, Halder RK, Kartazayeu U, Rosen RB, Gayen T, McCormick SA, Patel NS, Katz A, Perry HD, Paul M, RR. A. NIR laser tissue welding of in vitro porcine cornea and sclera tissue. Lasers Surg Med 2004; 35(4):293-303.
17. Menovsky T, Beek JF, van Gemert MJC. Laser tissue welding of dura mater and peripheral nerves: a scanning electron microscopy study. Lasers Surg Med 1996; 19(2):152-158.
18. Schober R, Ulrich F, Sander T, Durselen H, Hessel S. Laser-induced alteration of collagen substructure allows microscurgical tissue welding. Science 1986; 232(4756):1421-1422.
19. Tan HY, Teng SW, Lo W, Lin WC, Lin SJ, Jee SH, Dong CY. Characterizing the thermally induced structural changes to intact porcine eye, part 1: second harmonic generation imaging of cornea stroma. J Biomed Opt 2005; 10:540191-540195.
20. Matteini P, Ratto F, Rossi F, Cicchi R, Stringari C, Kapsokalyvas D, Pavone FS, Pini R. Photothermally-induced disordered patterns of corneal collagen revealed by SHG imaging. Optics Exp 2009; 17:4868-4878.
21. Matteini P, Sbrana F, Tiribilli B, Pini R. Atomic force microscopy and transmission electron microscopy analyses on low-temperature laser welding of the cornea. Lasers Med Sci 2009; 24:667-671.

22. Tang J, Godlewski G, Rouy S, Delacretaz G. Morphologic changes in collagen fibers after 830 nm diode laser welding. Lasers Surg Med 1997; 21(5):438-443.
23. Anderson RR, Lemole GM, Kaplan R, Solhpour S, Michaud N, Flotte T. Molecular mechanism of thermal tissue welding. Lasers Surg Med Suppl 1994; 6:56.
24. Hayashi K, Thabit Gr, Bogdanske JJ, Mascio LN, Markel MD. The effect of nonablative laser energy on the ultrastructure of joint capsular collagen. Arthroscopy 1996; 12:474-481.
25. Murray LW, Su L, Kopchok GE, White RA. Crosslinking of extracellular matrix proteins: a preliminary report on a possible mechanism of argon laser welding. Lasers Surg Med 1989; 9(5):490-496.
26. Rossi F, Pini R, Menabuoni L. Experimental and model analysis on the temperature dynamics during diode laser welding of the cornea. J Biomed Opt 2007; 12(1):014031.
27. Menabuoni L, Pini R, Rossi F, Lenzetti I, Yoo SH, Parel J-M. Laser-assisted corneal welding in cataract surgery: a retrospective study. J Cataract Refract Surg 2007; 33:1608-1612.
28. Rossi F, Matteini P, Ratto F, Menabuoni L, Lenzetti I, Pini R. Laser tissue welding in ophthalmic surgery. J Biophotonics 2008; 1:331-342.
29 Luca Buzzonetti, Paolo Capozzi, Gianni Petrocelli, Paola Valente, Sergio Petroni, Luca Menabuoni, Francesca Rossi, Roberto Pini.Laser Welding in Penetrating Keratoplasty and Cataract Surgery in Pediatric Patients. Early Results. J Cataract Refract Surg 2013 Dec; 39(12):1829-34. pii: S0886-3350(13)00981-4. doi: 10.1016/j.jcrs.2013.05.046.
30 Annalisa Canovetti, Alex Malandrini, Ivo Lenzetti, Francesca Rossi, Roberto Pini, Luca Menabuoni. Laser-assisted penetrating keratoplasty: one year's results in patients, using a laser-welded "anvil"-profiled graft. Accepted for publication in American Journal of Ophthalmology.

3.2 General References

31. D. Cabrera Fernández, PhD; A.M. Niazy, PhD, PE; R.M. Kurtz, MD; G.P. Djotyan, PhD; T. Juhasz, PhD. Biomechanical Model of Corneal Transplantation. Journal of Refractive Surgery Volume 22 March 2006
32. Florian Birnbaum & Antonia Wiggermann & Philip C. Maier & Daniel Böhringer & Thomas Reinhard.Clinical results of 123 femtosecond laser-assisted penetrating keratoplasties. Graefes Arch Clin Exp Ophthalmology. DOI 10.1007/s00417-012-2054-0
33. Sonia H. Yoo and Volkan Hurmeric. Femtosecond Laser-Assisted Keratoplasty. American Journal of Ophthalmology. February 2011, Volume 151, Issue 2, Pages 189–191.
34. Philip Maier, MD, Daniel Böhringer, MD, Florian Birnbaum, MD, and Thomas Reinhard, MD. Improved Wound Stability of Top-Hat Profiled Femtosecond Laser-Assisted Penetrating Keratoplasty In Vitro. The journal of cornea and external diseases. August 2012 - Volume 31 - Issue 8 - p 963–966.
35. Corneal transplantation. Donald T H Tan, John K G Dart, Edward J Holland, Shigeru Kinoshita. Lancet 2012; 379: 1749–61.